Computers and Concrete, *Vol. 14, No. 2 (2014) 127-143*
DOI: http://dx.doi.org/10.12989/cac.2014.14.2.127

Mechanical analysis for prestressed concrete containment vessels under loss of coolant accident

Zhen Zhou*, Chang Wu[a], Shao-ping Meng[b] and Jing Wu[c]

Southeast University, Key Laboratory of Concrete and Prestressed Concrete Structures of the Ministry of Education, Nanjing, 210096, China

(*Received August 10, 2012, Revised May 13, 2014, Accepted May 27, 2014*)

Abstract. LOCA (Loss Of Coolant Accident) is one of the most important utmost accidents for Prestressed Concrete Containment Vessel (PCCV) due to its coupled effect of high temperature and inner pressure. In this paper, heat conduction analysis is used to obtain the LOCA temperature distribution of PCCV. Then the elastic internal force of PCCV under LOCA temperature is analyzed by using both simplified theoretical method and FEM (finite element methods) method. Considering the coupled effect of LOCA temperature, a nonlinear elasto-plasitic analysis is conducted for PCCV under utmost internal pressure considering three failure criteria. Results show that the LOCA temperature distribution is strongly nonlinear along the shell thickness at the early time; the moment result of simplified analysis is well coincident with the one of numerical analysis at weak constraint area; while in the strong constrained area, the value of moments and membrane forces fluctuate dramatically; the simplified and numerical analysis both show that the maximum moment occurs at 6hrs after LOCA.; the strain of PCCV under LOCA temperature is larger than the one of no temperature under elasto-plastic analysis; the LOCA temperature of 6hrs has the greatest influence on the ultimate bearing capacity with 8.43% decrease for failure criteria 1 and 2.65% decrease for failure criteria 3.

Keywords: prestressed concrete containment vessel; loss of coolant accident; mechanical analysis; temperature distribution

1. Introduction

In recent years, nuclear electricity has been developed more and more extensively as a kind of clean energy. However, some large-scale nuclear leakage accidents happened in Chernobyl, Three-Miles Island and Fukushima has brought huge negative influence to the public environment, health, economics and society. Reactor's safety problem has been the most important research topic in the development of nuclear power.

Pressurized Water Reactor (PWR) is most extensively used for commercial purpose at present, with three protective barriers to prevent radiant matter from leaking into the surrounding environment. Prestressed Concrete Containment Vessel (PCCV) is the last and most important

*Corresponding author, Associate Professor, E-mail: seuhj@163.com
[a]Ph.D., E-mail: winslow_27@163.com
[b]Professor, E-mail: Cardoso_meng@sina.com
[c]Professor, E-mail: Wujing@vip.sina.com

http://www.techno-press.org/?journal=cac&subpage=8 ISSN: 1598-8198 (Print), 1598-818X (Online)

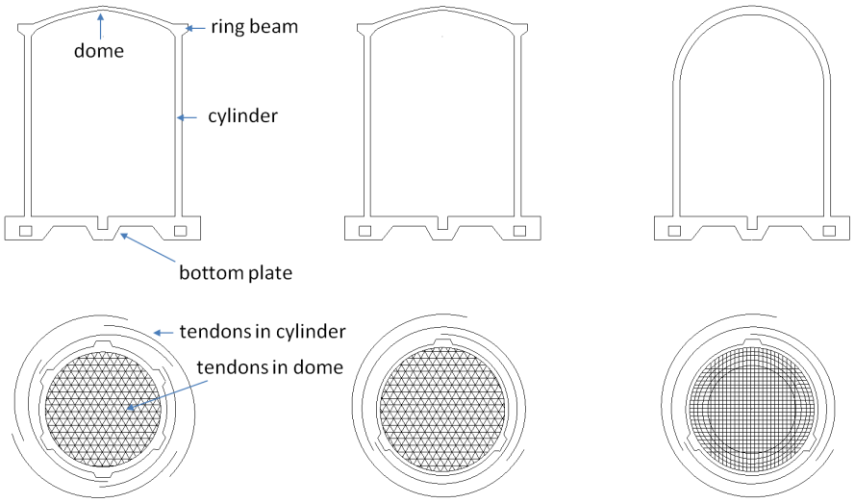

Fig. 1 Development of PCCV

In the first and second generation, shallow shell structure is adopted for the dome part, and ring beam is used between dome and cylinder to improve the connection stiffness. There are 6 buttresses in the cylinder of first generation PCCV, and 6 prestresssing tendons of 120 degree are set circumferentially. In the second generation PCCV, only 3 or 4 buttresses are used, with circumferentially set prestressing tendons of 240 or 360 degree. In the third generation PCCV, the shape of dome is changed from shallow shell to hemisphere and the ring beam is not adopted. Moreover, inverted-U-type tendon is adopted to combine the vertical tendon and dome tendon together. In China, the second generation PCCV is the most extensively used, such as Yangjiang nuclear power station in Guandong province, and Hongyan River nuclear power station in Liaoning province, which are still in construction presently.

The importance of PCCV has attracted many scholars and researchers to investigate its mechanical performance. Finite element method (FEM) is an important approach to research the performance of PCCV, in which axisymmetric shell element model or simplified solid element model are usually used by most scholars used (Byung and Se 2004, Ghavamian *et al*. 2007, Hu and Lin 2006). Noh *et al*. (2008) adopted both an axisymmetric model and a three-dimensional model to analyze a 1:4 scale model of a prestressed concrete containment vessel (PCCV) and the two models were refined by comparison of the analysis results with testing results. Yonezawa *et al*. (2003) discussed the accurate simulation method for prestress loss in PCCV by using the friction element. However, since there are a huge number of tendons in PCCV and every friction element need much computation, this method is difficult to be adopted into actual engineering. Lee (2011) developed a 9-node degenerated shell finite element program for ultimate pressure capacity evaluation and nonlinear analysis of a nuclear containment building. Song *et al*. (2009) developed a nonlinear volume control finite element method for the nonlinear analysis of PCCV to predict its ultimate internal pressure capacity. Cornish-Bowden *et al*. (2010) developed a method to determine the realistic residual prestress level in PCCV structures, taking into account in situ measurement results rather than design characteristics. Anderson *et al*. (2008) presented a reliability-based procedure to evaluate the prestress level of PCCV on the basis of data from in-service inspections, considering both the time dependent loss of prestress and the possibility of

tendons being broken (due to defects as corrosion). Berveiller *et al*. (2010) developed an effective method to estimate the long-term creep strains of PCCV by updating the evolution in time of a confidence interval on the creep strains.

Some research also focused on the safety evaluation under utmost accidents. Choi *et al*. (2008) estimated the seismic risk of a CANDU (Canada Deuterium Uranium) containment structure by performing the nonlinear seismic analysis for the near-fault earthquakes. Hirama *et al*. (2005) conducted a series of shaking table tests on a 1/8-scale reinforced concrete containment vessel model, with input motions corresponding to or exceeding a design earthquake assumed for a real nuclear power plant. Rao *et al*. (2010) carried out an uncertainty analysis of a PCCV structure subjected to an accidental pressure using a computational tool based on High Dimensional Model Representation (HDMR) that facilitates lower dimensional approximation of the original high dimensional implicit limit state/performance function. Al-Obaid (2011) conducted three-dimensional dynamics finite element analysis for PCCV under impact loads, including the non-linear behavior of concrete, structural damping and cracking. In his analysis, a combination of solid isoparametric, panel and line elements representing vessel concrete, steel lining, and prestressing tendons or conventional steel, respectively, was suggested. To evaluate the behavior of the advanced unbonded prestressed concrete containment vessel (UPCCV) for one typical China nuclear power plant under Japan's March 11 earthquake, Duan *et al*. (2014) carried out five nonlinear time history analysis and a nonlinear static analysis for a 1:10 scale UPCCV structure with MSC. MARC finite element program.

LOCA (Loss of Coolant Accident) is one of the most important utmost accidents. Although the possibility of LOCA is pretty low, the internal pressure would be increased greatly when it happens. At the same time, the temperature will also increase dramatically and changes continuously with time. This will threaten the safety of PCCV structure. Most researches only consider the influence of increasing pressure, while the LOCA temperature influence are few investigated. In this paper, heat conduction analysis is used to obtain the LOCA temperature distribution of PCCV. Then the elastic internal force of PCCV under LOCA temperature is analyzed by using both simplified theoretical method and accurate FEM method. Considering the coupled effect of LOCA temperature, a nonlinear elasto-plasitic analysis is conducted for PCCV under utmost internal pressure, to evaluate the influence of LOCA temperature on ultimate pressure capacity of PCCV.

2. LOCA temperature distribution in shell wall

2.1 basic assumptions

The LOCA temperature distribution in the shell wall, $T(x, \tau)$, is supposed to be the function of x (radial location along the shell thickness from inner surface) and τ (time). $T(x, \tau)$ should consist of two parts. One is the existent temperature distribution before LOCA happens, generated by the exterior environmental and interior operation temperatures, and can be attributed to the stable heat conduction problem which is not related to time. Therefore, its function can be supposed as $T_1(x)$. The other is the temperature change caused by LOCA. Since LOCA is occasional and sudden, and relevant cooling measures would be adopted after it happen, this can be attributed to non-stable heat conduction problem which is time-related. Therefore, its function can be supposed as $T_2(x, \tau)$.

Then the total temperature distribution in shell wall under LOCA can be written as following:

$$T(x,\tau)=T_1(x)+T_2(x,\tau) \tag{1}$$

Since the diameter of PCCV is large, and the shell thickness is greatly smaller than diameter and height, the temperature distribution problem can be analyzed using one-dimension heat conduction analysis.

2.2 The existent temperature distribution before LOCA

According to stable heat conduction theory, the one-dimension differential equation is as following:

$$\frac{d^2T_1}{dx^2}=0 \tag{2}$$

The exterior environmental temperature is usually known, so the boundary condition for this problem can use the third boundary conditions in heat transfer theory. That is: the convection heat transfer coefficient between the boundary surface and surrounding fluid (α) and the fluid temperature (T_f) are known, then the boundary conditions can be expressed as:

$$-\lambda\left.\frac{dT_1}{dx}\right|_{x=0}=\alpha_1\left(T_{f1}-T_{w1}\right) \tag{3}$$

$$-\lambda\left.\frac{dT_1}{dx}\right|_{x=\delta}=\alpha_2\left(T_{w2}-T_{f2}\right) \tag{4}$$

where T_{f1}, T_{f2} are the interior and exterior atmosphere temperature; T_{w1}, T_{w2} are the inner and outer surface temperature of shell wall, i.e., $T_1|_{x=0}=T_{w1}$, $T_1|_{x=0}=T_{w2}$ (δ is the shell wall thickness); λ is the heat conduction coefficient; α_1, α_2 are the convection heat transfer coefficient between the inner, outer surface and surrounding fluid, respectively.

For the heat conduction problem with constant material property, the temperature gradient in the shell wall is constant as following:

$$\frac{dT_1}{dx}=-\frac{T_{w1}-T_{w2}}{\delta} \tag{5}$$

Therefore, the temperature distribution is linear in the shell wall as following:

$$T_1(x)=T_{w1}-\frac{T_{w1}-T_{w2}}{\delta}x \tag{6}$$

The key is to solve T_{w1} and T_{w2}. According to Fourier law, the heat flux is:

$$q=-\lambda\frac{dT_1}{dx} \tag{7}$$

So Eqs. (3)-(5) can be rewritten as:

$$q\big|_{x=0} = \alpha_1\left(T_{f1} - T_{w1}\right) \tag{8}$$

$$q = \frac{\lambda}{\delta}\left(T_{w1} - T_{w2}\right) \tag{9}$$

$$q\big|_{x=\delta} = \alpha_2\left(T_{w2} - T_{f2}\right) \tag{10}$$

In the stable heat conduction process, there is:

$$q\big|_{x=0} = q = q\big|_{x=\delta} \tag{11}$$

Then Eqs. (8) - (10) can be combined as:

$$q = \frac{T_{f1} - T_{f2}}{\frac{1}{\alpha_1} + \frac{\delta}{\lambda} + \frac{1}{\alpha_2}} \tag{12}$$

The heat flux solved by Eq. (12) can be substituted into Eqs. (8)-(10) to solve T_{w1} and T_{w2}. Then the existent temperature distribution before LOCA can be obtained.

To superpose to the temperature field after LOCA, the coordination origin of initial temperature distribution should be set to T_1=T_{w1}. Then Eq. (6) can be rewritten as:

$$T_1\left(x\right) = -\frac{T_{w1} - T_{w2}}{\delta}x \tag{13}$$

2.3 The temperature distribution after LOCA

The temperature distribution without considering the initial heat conduction is first solved. The temperature in the shell wall is supposed to be T_{w1} uniformly before LOCA. After LOCA, the inner surface temperature of shell wall is equivalent to the environmental temperature inside PCCV, which is a time-related function supposed as $T_w(\tau)$ (τ denotes the time after LOCA). The heat conduction differential equation to describe this problem is as following:

$$\frac{\partial T_2}{\partial \tau} = \alpha \frac{\partial^2 T_2}{\partial x^2} \tag{14}$$

where $\alpha=\lambda/\rho$; ρ is the density of concrete. The boundary condition is:

$$T_2\left(x,0\right) = T_{w1} \;;\; T_2\left(0,\tau\right) = T_w\left(\tau\right) \;;\; T_2\left(\infty,\tau\right) = T_{w1} \tag{15}$$

According to the Laplace transformation, the solution can be obtained ayiq following:

$$\frac{T_2 - T_w}{T_{w1} - T_w} = \frac{2}{\sqrt{\pi}} \int_0^{\frac{x}{2\sqrt{a\tau}}} e^{-\eta^2} d\eta = erf\left(\frac{x}{2\sqrt{a\tau}}\right) \tag{16}$$

Eq. (16) can be rewritten as:

$$T_2(x,\tau) = T_w + (T_{w1} - T_w) \cdot erf\left(\frac{x}{2\sqrt{a\tau}}\right) \tag{17}$$

where *erf*(*x*) is named as "error function" in mathematics.

Then the total LOCA temperature distribution can be obtained by superpose Eq. (13) and Eq. (17) as following:

$$T(x,\tau) = T_1(x) + T_2(x,\tau) = T_w + (T_{w1} - T_w) \cdot erf\left(\frac{x}{2\sqrt{a\tau}}\right) - \frac{T_{w1} - T_{w2}}{\delta} x \tag{18}$$

2.4 Example analysis

The second generation PCCV is shown in Fig. 2. The geometric parameters are as following: the inner radius of the cylinder shell is 18.5m; the radius of the shallow dome shell is 24m and its central angle is 86°; the shell thickness is 0.9m; the total height of PCCV is 68.534m. The material parameters are: the strength grade of concrete is C50; the elastic modulus of concrete is 3.45×10^4MPa and the poisson ratio is 0.2; the density of concrete is 2500kg/m^3. The thermal parameters include: the thermal expansion coefficient is 10^{-5}/℃; the heat conduction coefficient is 2.3w/(m·℃); the heat capacity is 1000J/kg℃; the convection heat transfer coefficient between the inner, outer surface and surrounding fluid is 8W/(m^2·℃) and 16W/(m^2·℃), respectively. Supposing that the internal and external atmosphere temperature is 38℃ and 5℃, respectively, the heat flux can be solved as q=49.57W/m^2 according to Eq. (12). Then according to Eq. (7) and Eq. (9), the inner and outer surface temperature of shell wall can be solved as T_{w1}=31.8℃ and T_{w2}=8.1℃. Therefore, the following equation can be obtained:

$$T_1(x) = -\frac{T_{w1} - T_{w2}}{\delta} x = -\frac{24}{0.9} x$$

Similarly, substitute the material and thermal parameters into Eq. (17), the following equation can be obtained:

$$T(x,\tau) = T_w(\tau) + \left[32 - T_w(\tau)\right] \cdot erf\left(\frac{x}{2\sqrt{a\tau}}\right) - \frac{24}{0.9} x$$

According to the relevant literature (Zhao *et al*. 2003), the atmosphere temperature inside PCCV at different time after LOCA, $T_w(\tau)$, has been analyzed as shown in Table 1.

Table 1 Atmosphere temperature inside PCCV at different time after LOCA

Time	10 min	30 min	6 hrs	12 hrs	24 hrs
Temperature (^{o}C)	145	130	120	100	80

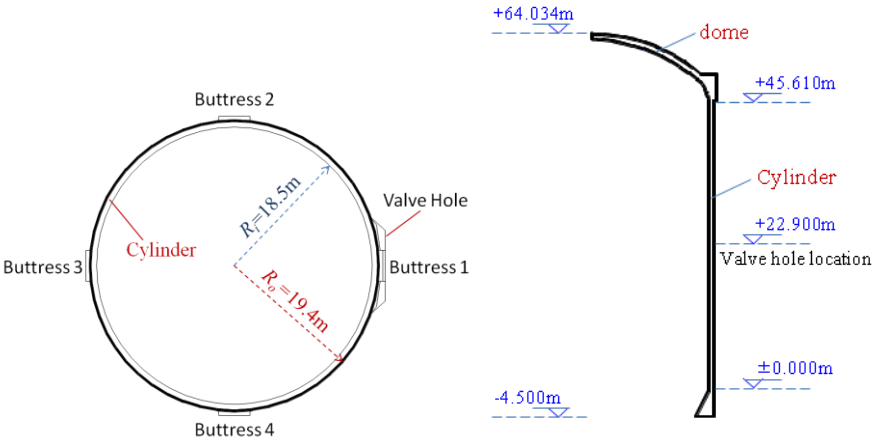

Fig. 2 Geometry of second generation PCCV

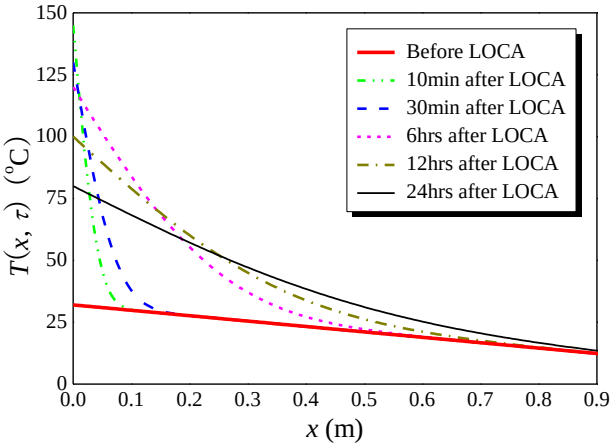

Fig. 3 LOCA temperature distribution along the shell thickness direction at different time

Substitute the data of $T_w(\tau)$ in Table 1 into Eq. (18), the LOCA temperature distribution along the shell thickness direction at different time can be obtained, as shown in Fig.3. It can be seen that the LOCA temperature distribution is strongly nonlinear along the shell thickness at the early time after LOCA. With time passing, the temperature near the inner shell surface decrease, while the one near the outer surface increase. It means the temperature distribution along the shell thickness becomes more uniform and its nonlinearity is gradually weakened.

3. Elastic analysis of PCCV under LOCA temperature

1. Simplified analysis

The internal force in the structure caused by temperature action is related with the constraint degree. The constraint can be divided into two parts: internal constraint and external constraint.

For the second generation PCCV, the external constraint is relatively strong near bottom plate, including circumferential and vertical constraint. At the junction area between dome and cylinder, internal constraint is relatively strong. At other locations, the circumferential and vertical constraint is relatively weak. Therefore, compared with strong constrained area, the vertical and circumferential axial force at most weak constrained locations should be close to zero (this can be verified through the later numerical analysis). The internal force of PCCV is mainly the moment caused by internal constraint effect under the temperature difference between inner and outer shell surface, including radial and circumferential moment.

To conduct the simplified analysis for PCCV, the constraint effect near the bottom plate is not considered and the axial force in shell wall under LOCA temperature is supposed to be zero. Then the simplified calculation method for the moment in shell wall is deduced. Suppose the temperature difference distribution function is:

$$\Delta T(x,\tau) = T(x,\tau) - T_c \tag{19}$$

where T_c is the construction temperature of PCCV). The circumferential strain (ε_{c1}) and vertical stain (ε_{v1}) can be expressed as:

$$\varepsilon_{c1}(x,\tau) = \varepsilon_{v1}(x,\tau) = -C_T \cdot \Delta T(x,\tau) \tag{20}$$

where C_T is thermal expansion coefficient. At the locations far from bottom plate, the external constraint is relatively weak. However, for the existence of internal constraint, the shell wall section can still be freely expanded and the plane section assumption can be approximately met. Therefore, the internal constraint strain is caused as follows:

$$\varepsilon_c(x,\tau) = \varepsilon_{c1}(x,\tau) - \varepsilon_{cm}(\tau) \quad , \quad \varepsilon_v(x,\tau) = \varepsilon_{v1}(x,\tau) - \varepsilon_{vm}(\tau) \tag{21}$$

where ε_{cm} and ε_{vm} are calculated as:

$$\varepsilon_{cm}(\tau) = \frac{1}{\delta}\int_0^{\delta} \varepsilon_{c1}(x,\tau)dx \quad , \quad \varepsilon_{vm}(\tau) = \frac{1}{\delta}\int_0^{\delta} \varepsilon_{v1}(x,\tau)dx \tag{22}$$

According to the elastic mechanics theory, the circumferential stress (σ_c) and vertical stress (σ_v) can be obtained as:

$$\sigma_c(x,\tau) = \frac{E}{1-\mu^2}\left[\varepsilon_c(x,\tau) + \mu\varepsilon_v(x,\tau)\right] \tag{23}$$

$$\sigma_v(x,\tau) = \frac{E}{1-\mu^2}\left[\varepsilon_v(x,\tau) + \mu\varepsilon_c(x,\tau)\right] \tag{24}$$

where E is elastic modulus; μ is poisson ratio. Substitute Eq. (21) into Eq. (23) and Eq. (24), the following equation can be obtained:

Table 2 The moment in shell wall at different time after LOCA

Time	10 min	30 min	6 hrs	12 hrs	24 hrs
Moment (MN·m/m)	1.381	1.562	2.536	2.422	1.856

$$\sigma_c(x,\tau)=\sigma_v(x,\tau)=-\frac{E\alpha(\Delta T-\Delta T_m)}{1-\mu} \tag{25}$$

where:

$$\Delta T_m=\frac{1}{\delta}\int_0^{\delta}\Delta T(x,\tau)dx$$

Then the circumferential moment (M_c) and vertical moment (M_v) in the shell wall under temperature action is:

$$M_c=M_v=\int_0^{\delta}\sigma(x,\tau)\cdot\left(\frac{\delta}{2}-x\right)dx=\frac{E\alpha}{1-\mu}\int_0^{\delta}\left[\Delta T(x,\tau)-\Delta T_m(\tau)\right]\cdot\left(\frac{\delta}{2}-x\right)dx \tag{26}$$

Since the LOCA temperature distribution in shell wall is strongly nonlinear, the section should be equally divided into *n* segments along the shell wall thickness direction. Then the moment can be calculated by superposition as:

$$M_c=M_v=\frac{E\alpha}{1-\mu}\sum_{k=1}^{n}\left[\Delta T_k(x,\tau)-\Delta T_m(\tau)\right]\cdot d_k\cdot\Delta\delta \tag{27}$$

where:

$$\Delta T_k=\frac{\Delta T(x_{k-1},\tau)+\Delta T(x_k,\tau)}{2}\qquad (k=0,\ 1,\ 2,\ \ldots,\ n)$$

$$d_k=\frac{\delta}{2}-\frac{(x_{k-1}+x_k)}{2},\quad x_k=k\cdot\Delta\delta,\quad \Delta\delta=\frac{\delta}{n}$$

According to the LOCA temperature distribution function solved in section 2.4, the moment in shell wall at different time after LOCA can be calculated using Eq. (25), as shown in Table 2. It can be seen that the maximum moment happens at 6hrs after LOCA, although the temperature at this time is not the highest. The main reason is that the temperature distribution at the early time (10min and 30min) focuses on the area near inner shell surface, while the temperature at most locations along the shell wall thickness are very low. So the influence of the high temperature at this time is very limited and the moment caused by temperature action is relatively smaller.

3.2 Numerical analysis

To conduct an accurate analysis, a numerical model of PCCV is established using finite element software ABAQUS, as shown in Fig. 4. There are 6 holes in the cylinder, including 1 valve hole, 2

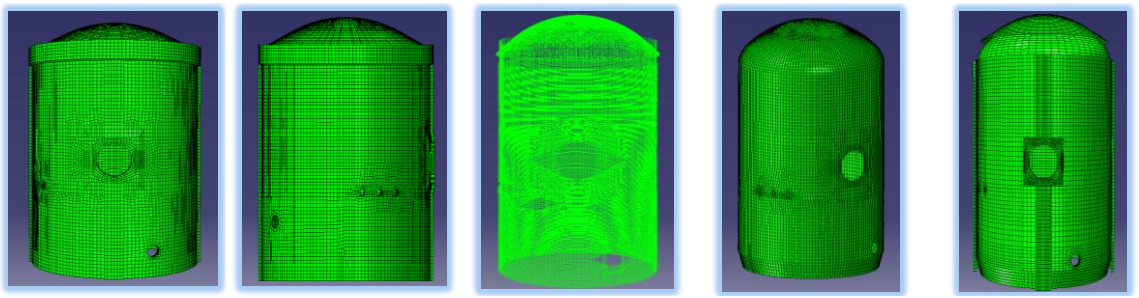

(a) Front view (b) Side view (c) Tendon (d) Steel liner (e) Reinforcement

Fig. 4 Numerical model of PCCV in ABAQUS

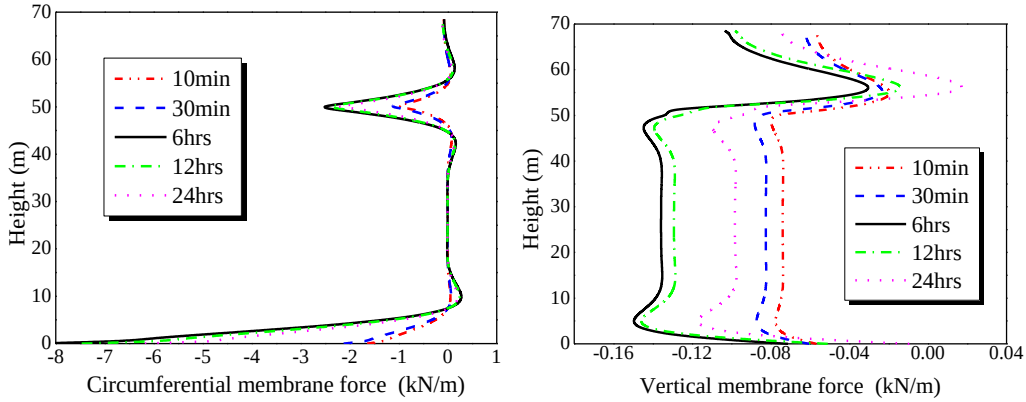

Fig. 5 Membrane force distribution along height direction at different time after LOCA

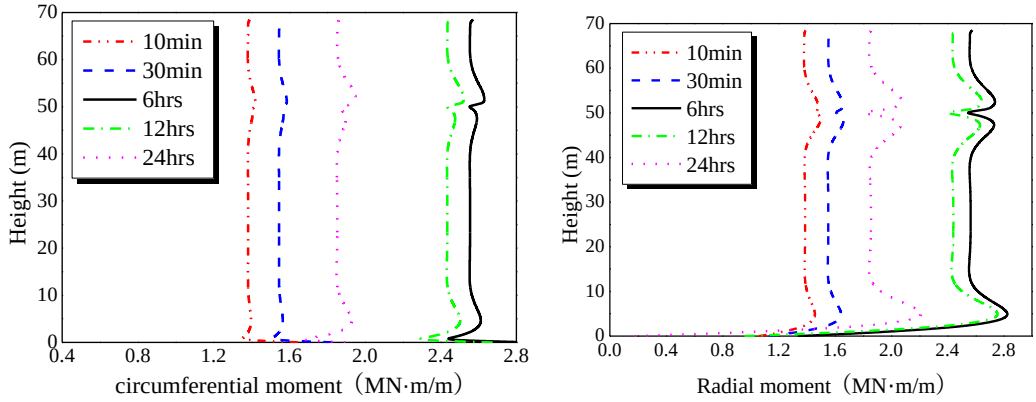

Fig. 6 Membrane force distribution along height direction at different time after LOCA

Table 3 Moment results comparison of numerical and simplified analysis (MN·m/m)

Time		10 min	30 min	6 hrs	12 hrs	24 hrs
Simplified analysis		1.375	1.562	2.526	2.412	1.846
Numerical analysis	Radial moment	1.382	1.546	2.555	2.435	1.853
	Circumferential moment	1.387	1.552	2.564	2.441	1.849

human hole and 3 small holes. The cylinder near valve hole is thickened to prevent from cracking too early. Four buttresses are set in the horizontal section with the mutual angel is 90°. Two layers of circumferential and one layer of vertical prestressing tendons are set in the cylinder wall. The top of vertical tendons is anchored on the upper surface of ring beam while the bottom anchored on the bottom plate. Circumferential tendons are anchored to buttresses. In the dome shell, three layers of prestressing tendons are set to be anchored on the external side of ring beam. Three layers of circumferential and vertical reinforcements are set in the cylinder and dome. Moreover, one layer of steel liner with the thickness 6mm is set in the whole inner shell surface. The steel linear is anchored tightly with the concrete part of PCCV to form an integral structure. In ABAQUS simulation, solid element C3D8 is used for concrete part, truss element T3D2 for prestressing tendons, membrane element for reinforcement layer, and shell element S4 for steel liner. The prestressing tendon elements are separately constructed and then embedded into the concrete elements through the function "embedded region" provided by ABAQUS to make them work together.

For the elastic internal force analysis of PCCV under LOCA temperature, the prestress effect is not considered, which will be included in the later elasto-plastic analysis under LOCA temperature and inner pressure. The analysis results are shown in Fig. 5 and Fig. 6.

As shown in Fig.5, compared with the force in the strong constraint area (near bottom plate and ring beam), the circumferential membrane force of most locations and the vertical membrane force are relatively small and close to zero. However, the membrane forces in the strong constraint area fluctuate dramatically, for the strong constraint effect. For the moment result, as shown in Fig.5, the moment value at most locations are relatively uniform while the values in strong constrained area change distinctly. According to the elastic mechanics theory, the strong constraint effect exist within the distance of $2.5\sqrt{R\delta} \approx 10\text{m}$ from constraint end (R is the radius of the cylinder shell), which can be clearly seen in Fig. 6. The maximum moment occurs at 6hrs after LOCA, which is in accordance with the simplified analysis results in section 3.1. Therefore, in the PCCV elastic design, 6hrs after LOCA can be considered as one of the control load cases. Comparison between the moment of numerical analysis and simplified analysis at weak constraint area are shown in Table 3. It can be seen that the simplified result is well coincident with the numerical analysis.

4. Elasto-plastic analysis of PCCV under LOCA temperature and inner pressure

4.1 Constitutive relation of material

In ABAQUS, two material models can be used to simulate the nonlinear behavior of concrete material, including smeared crack model (SCM) and damaged plasticity model (DPM). In this paper, DPM is employed for the concrete part of PCCVs, since it is easier to converge and get reliable solution results than SCM. In DPM, the inelastic behavior of concrete is represented by combing isotropic damage and isotropic tension/compression plasticity. The uniaxial compressive and tensile stress-strain relation of concrete is necessary for DPM, which can be determined according to China Concrete Structural Design Code (2002) (shown in Fig. 7). To improve the stability in solution process, the curved stress-strain relation is simplified to multi-linear simulation. The reinforcements in PCCV including two categories: Grade II and Grade III. A double linear ideal elasto-plastic stress-strain relation is used for reinforcement, steel liner and prestressing tendons. The yield stress and strain are shown in Table

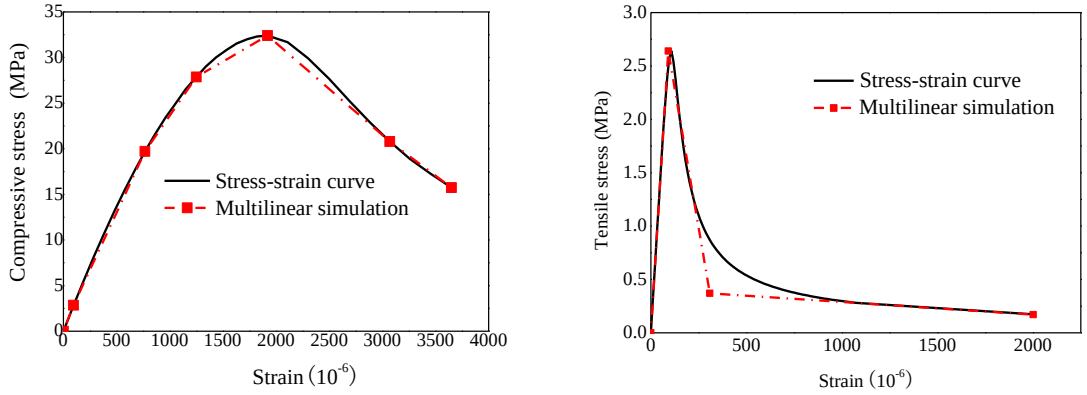

(a) compressive (b) tensile

Fig. 7 Uniaxial stress-strain curve of concrete (C50)

Table 4 Yield stress and strain of reinforcement, steel liner and prestressing tendons

Material	Reinforcement		Steel liner	Prestressing tendon
	GradeII	Grade III		
Yield stress(MPa)	335	400	320	1507
Yield strain($\times 10^{-6}$)	1680	2000	1520	7930

4.2 Determination of prestress

As shown in Fig. 8, horizontal circumferential tendons in cylinder include inner ring (radius 19.03m) and outer ring (radius 19.23m). Horizontal tendons are stretched at both ends. Vertical tendons in cylinder is stretched on the top surface of ring beam. Tendons in dome are stretched at both ends on the outer surface of ring beam. Considering 60 years of prestress loss, the effective prestress retained in tendons after stretched are calculated as shown in Fig. 9, according to "Eurocode 2: Design of concrete structures" (EN 1992-1-1:2004).

In ABAQUS, decreasing temperature method is adopted to simulate the prestress effect. At this time, the effective prestress retained in tendons should be transformed into equivalent temperature, as follows:

$$\Delta T_s = \frac{\sigma_s}{E_s \cdot \alpha_s} \tag{28}$$

where σ_s is the effective prestress; E_s, α_s is the elastic modulus and thermal expansion coefficient of tendons. It should be noted that if ΔT_s in Eq. (28) is directly used in simulation, the actual stress in tendons could be less than σ_s for the coordinated deformation of concrete and tendons. This may lead to an inaccurate result. Therefore, the following iterative modification equation is adopted:

$$[\Delta T_s^{(n)}] = \frac{[\sigma_s]}{[S^{(n-1)}]} \cdot [\Delta T_s^{(n-1)}] \tag{29}$$

where $\Delta T_s^{(n)}$ and $\Delta T_s^{(n-1)}$ is the calculated equivalent temperature after n^{th} and $(n\text{-}1)^{\text{th}}$ iteration, respectively; $S^{(n-1)}$ is the actual stress in tendons when $\Delta T_s^{(n-1)}$ is used for tendons.

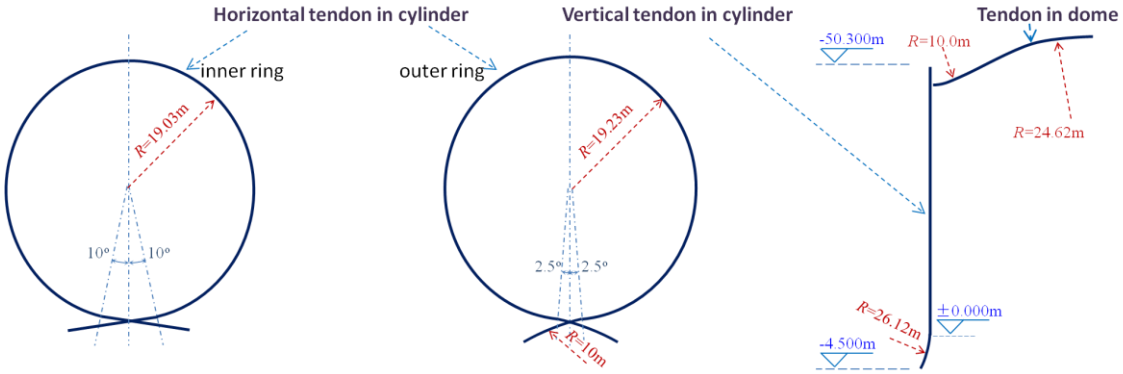

Fig. 8 Geometry of prestressing tendons

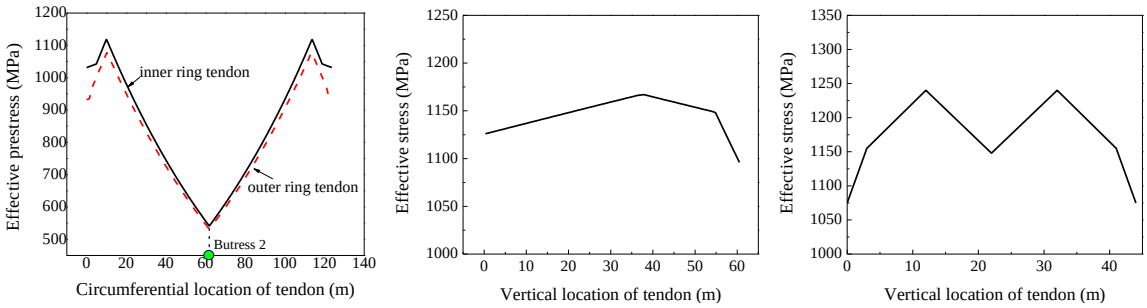

(a) Horizontal tendons (b) Vertical tendons (c) Tendons in dome

Fig. 9 Effective prestress retained in tendons

4.3 Failure criteria

According to the function of PCCV, the strength and sealing performance should be ensured under great internal pressure. Some experiments has revealed that the cylinder always reaches plastic deformation earlier than the dome. Therefore, the failure state and criteria is mainly determined by concrete cylinder and steel liner. At present, three failure criteria are usually used for the elasto-plastic limit states analysis of PCCV:

Criteria 1: Maximum tensile strain of concrete cylinder reaches 10000×10^{-6}

Criteria 2: Maximum strain of steel liner reaches the tearing strain 0.2

Criteria 3: Most tendons in cylinder yields (stress reaches 1507MPa)

4.4 Analysis result

In present elasto-plastic analysis of PCCV, only internal pressure load is considered. The internal pressure is increased gradually based on the design pressure, until the stress state of PCCV reaches the failure criteria. Then, the internal pressure at this time is taken as the limit ultimate bearing capacity. However, PCCV subjects to high temperature action as well as great internal pressure under LOCA. The elasto-plastic analysis only considering internal pressure can not reflect the real stress state of PCCV under LOCA. Therefore, the LOCA temperature distribution at

different time is considered in the elasto-plastic analysis. The total analysis is divided into two steps. In the first step, the stress state of PCCV under self-weight, prestress and LOCA temperature is calculated. Then based on the results of step 1, the internal pressure is applied to the inner surface of steel liner, with the value gradually increasing from 0 to 3 times of design pressure, i.e., $3P_a$=1.26MPa (P_a=0.42MPa is the design pressure).

The elasto-plastic analysis results under differential LOCA temperature are shown in Figs. 10-12. As shown in Fig. 10, the radial displacement increase linearly when the internal pressure is small. At this time, the whole PCCV structure is basically in the elastic stress state. With the increase of internal pressure, the displacement increase more and more rapidly. It indicates that some part of cylinder has reached the plastic strain and the plastic area is gradually being extended. When LOCA temperature is considered, the displacement develops more rapidly. This means that the cylinder reaches the plastic strain earlier. The displacement under 6hrs LOCA temperature case is a little larger than the other LOCA temperature cases.

Fig. 11 and Fig. 12 show the circumferential and vertical strain of the point near valve hole at the elevation 22.9m. It can be seen that on the inner shell surface, the circumferential strain under LOCA temperature develops faster than the no temperature result before 1.0MPa internal pressure. When internal pressure exceeds 1.0MPa, the circumferential strain of no temperature is larger. It indicates that although the cylinder reaches circumferential plastic strain earlier when LOCA temperature considered, the circumferential plastic strain develops more gradually. Compared with the circumferential strain, the vertical strain on the inner shell surface is relatively small which has little influence on the failure state of PCCV. On the outer shell surface, the circumferential strain under LOCA temperature is distinctly larger than the one of no temperature. It means the

LOCA temperature has greater influence on the circumferential strain development on the outer shell surface. The vertical strain on the outer shell surface under LOCA temperature is a little larger than the no temperature result. Totally speaking, the strain under LOCA temperature is larger than the one of no temperature, and results of 6hrs LOCA temperature is the maximum.

According to the three failure criteria in section 4.3, the ultimate bearing capacity under different LOCA temperature distribution is shown in Table 5. It can be seen that when the LOCA temperature is considered, the ultimate bearing capacity of PCCV is reduced. The LOCA temperature of 6hrs has the greatest influence on the ultimate bearing capacity with 8.43% decrease for criteria 1 and 2.65% decrease for criteria 3.

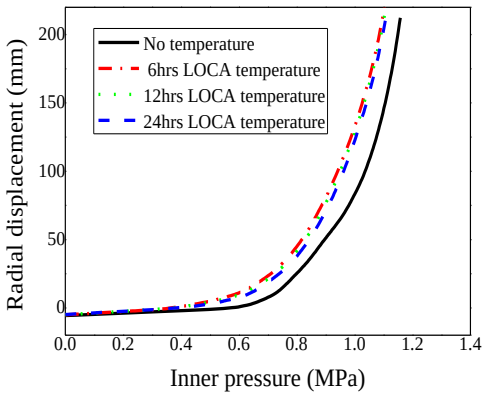

Fig. 10 Radial displacement of the point near valve hole at the elevation 22.9m

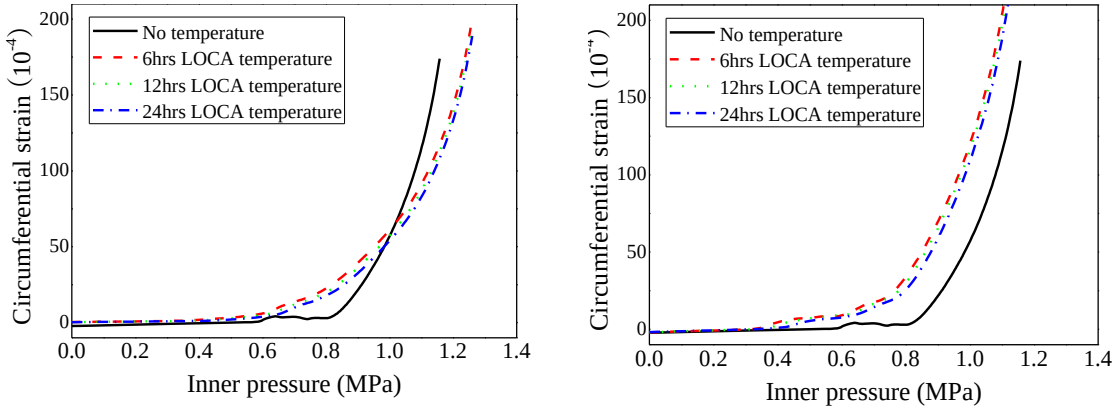

(a) Inner shell surface (b) Outer shell surface

Fig. 11 Circumferential strain of the point near valve hole at the elevation 22.9m

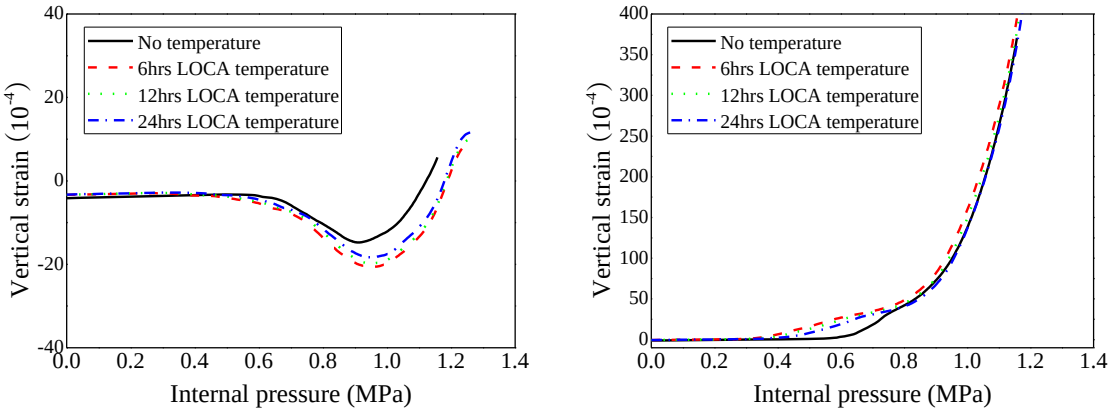

(a) Inner shell surface (b) Outer shell surface

Fig. 12 Vertical strain of the point near valve hole at the elevation 22.9 m

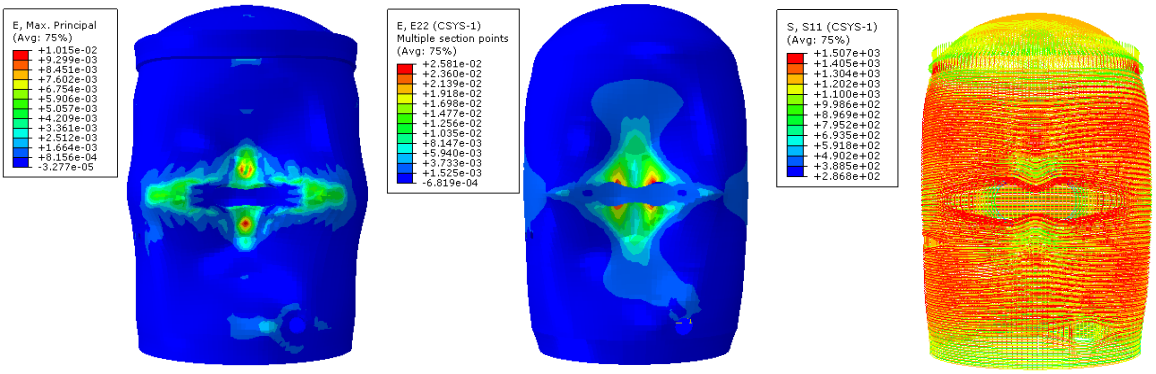

(a) criteria 1: concrete strain (b) criteria 2: steel liner strain (c) criteria 3: stress in tendons

Fig. 13 Stress state of PCCV at the limited failure state of 6hrs LOCA temperature

Table 5 The Ultimate bearing capacity under different LOCA temperature distribution

Failure criteria	Ultimate bearing capacity (MPa)			
	No temperature	6hrs LOCA temperature	12hrs LOCA temperature	24hrs temperature
Criteria 1	0.83	0.76	0.78	0.81
Criteria 2	>1.26	>1.26	>1.26	>1.26
Criteria 3	1.13	1.1	1.109	1.113

The stress state of PCCV at the limited failure state of 6hrs LOCA temperature is shown in Fig. 13. It can be seen that the maximum concrete strain and steel liner strain are focuses near the valve hole. For criteria 1, structural failure is originated from a small area below the valve hole, while it is from the edge of vale hole for criteria 2. For criteria 3, most horizontal circumferential tendons yield, while the vertical tendons in cylinder and tendons in dome do not yield. It also indicates that the horizontal circumferential tendons play a greatly important role to resist the increasing internal pressure.

5. Conclusions

(1) The LOCA temperature distribution is strongly nonlinear along the shell thickness at the early time after LOCA. With time passing, the temperature near the inner shell surface decrease, while the one near the outer surface increase. It means the temperature distribution along the shell thickness becomes more uniform and its nonlinearity is gradually weakened. Therefore, in the design of PCCV, the real LOCA temperature distribution at different time should be considered to obtain accurate and safety mechanical analysis result.

(2) The moment result of simplified analysis is well coincident with the one of numerical analysis at weak constraint area. While in the strong constrained area, the value of moments and membrane forces fluctuate dramatically. The simplified and numerical analysis both show that the maximum moment occurs at 6hrs after LOCA. Therefore, in the PCCV elastic design, 6hrs after LOCA can be considered as one of the control load cases.

(3) Elasto-plastic analysis shows that the strain of PCCV under LOCA temperature is larger than the one of no temperature, and results of 6hrs LOCA temperature is the maximum. When the LOCA temperature is considered, the ultimate bearing capacity of PCCV is reduced. The LOCA temperature of 6hrs has the greatest influence on the ultimate bearing capacity with 8.43% decrease for criteria 1 and 2.65% decrease for criteria 3.

Acknowledgment

This research is sponsored by “Jiangsu Province Natural Science Foundation of China” (BK2010428), “the Fundamental Research Funds for the Central Universities” and “A Project Funded by the Priority Academic Program Development of Jiangsu Higher Education Institutions” (PAPD). The supports are gratefully acknowledged.

References

Al-Obaid, Y.F. (2011), "Finite element cracking analysis of nuclear containment vessels under external Impacts", *Proceeding of the ASME Small Modular Reactors Symposium*, Washington, DC, SEP.

Anderson, P., Hansson, M. and Thelandersson, S. (2008), "Reliability-based evaluation of the prestress level in concrete containments with unbonded tendons", *Struct. Saf.*, **30**(1), 78-89

Berveiller, M., Le pape, Y. and Sudret, B. (2012), "Updating the long-term creep strains in concrete containment vessels by using Markov chain Monte Carlo simulation and polynomial chaos expansions", *Struct. Infrastruct. E.*, **8**(5), 425-440

Byung, H.O. and Se, J.J. (2004), "Advanced automatic generation scheme of prestressing tendons for efficient FE analysis of PSC shell structures", *Finite. Elem. Anal. Des.*, **40**(8), 913-931.

Choi, I.K., Choun, Y.S. and Ahn, S.M. (2008), "Probabilistic seismic risk analysis of CANDU containment structure for near-fault earthquakes", *Nucl. Eng. Des.*, **238**(6), 1382-1391.

Cornish-Bowden, I., Thillard, G. and Capra, B. (2010), "Prediction of prestressing losses for long term operation of nuclear reactor buildings", *Proceeding of the International Workshop on Ageing Management of Nuclear Power Plants and Waste Disposal Structures (AMP)*, Toronto, Nov.

Duan, A., Zhao, Z.Z., Chen, J., Qian, J.R. and Jin, W.L. (2014), "Nonlinear time history analysis of a prestressed concrete containment vessel model under Japan", *Comput. Concret*, **13**(1), 1-16

Ghavamian, S., Courtois, A. and Valfort, J.L. (2007), "Mechanical simulations of SANDIA II tests OECD ISP 48 bench mark", *Nucl. Eng. Des.*, **237**(12-13), 1406-1418.

Hirama, T., Goto, M., Shiba, K., Kobayashi, T., Tanaka, R., Tsurumaki, S., Takiguchi, K. and Akiyama, H. (2005), "Seismic proof test of a reinforced concrete containment vessel (RCCV) - Part 2: Results of shaking table tests", *Nucl. Eng. Des.*, **235**(13), 1349-1371

Hu, H.T. and Lin, Y.H. (2006), "Ultimate analysis of PWR prestressed concrete containment subjected to internal pressure original research article", *Int. J. Pres. Ves. Pip.*, **83**(3), 161-167

Lee, H.P. (2011), "Shell finite element of reinforced concrete for internal pressure analysis of nuclear containment building", *Nucl. Eng. Des.*, **241**(2), 515-525

Noh, S.H., Moon, I.H. and Lee, J.B. (2008), "Analysis of prestressed concrete containment vessel (PCCV) under severe accident loading", *Nucl. Eng. Technol.*, **40**(1), 77-86

Rao, B.N., Chowdhury, R., Meher Prasad, A., Singh, R.K. and Kushwaha, H.S. (2010), "Reliability analysis of 500 MWe PHWR inner containment using high-dimensional model representation", *Int. J. Pres. Ves. Pip.*, **87**(5), 230-238

Song, H.W., Na, S.H., Shim, B. and Kim, S.H. (2009), "Path-dependent nonlinear analysis of a concrete reactor containment vessel subjected to internal pressure using a volume control technique", *Eng. Struct.*, **31**(4), 990-998

Yonezawa, K., Imoto, K., Ohba, M., Ikeuchi, T., Kozuma, M., Murazumi, Y. and Sato, K. (2003), "Analytical study on structural failure mode of 1/4 PCCV test model", *Proceeding Transactions of the 17th International Conference on Structural Mechanics in Reactor Technology*, Prague, Nov.

Zhao, J., Yu, H.X. and Li, F. (2003), "Calculation and analyses of containment pressure and temperature for PWR 1000XL", *Nucl. Power. Eng.*, **24**(5), 410-411. (in Chinese)